Anisotropy of heat conduction in Mo/Si multilayers

V. V. Medvedev,[1,a)] J. Yang,[2] A. J. Schmidt,[2] A. E. Yakshin,[1] R. W. E. van de Kruijs,[1] E. Zoethout,[3] and F. Bijkerk[1]
[1]*MESA+ Institute for Nanotechnology, University of Twente, P.O. Box 217, 7500 AE Enschede, The Netherlands*
[2]*Department of Mechanical Engineering, Boston University, Boston, Massachusetts 02215, USA*
[3]*FOM Institute DIFFER, Eindhoven, The Netherlands*

(Received 8 June 2015; accepted 8 August 2015; published online 24 August 2015)

This paper reports on the studies of anisotropic heat conduction phenomena in Mo/Si multilayers with individual layer thicknesses selected to be smaller than the mean free path of heat carriers. We applied the frequency-domain thermoreflectance technique to characterize the thermal conductivity tensor. While the mechanisms of the cross-plane heat conduction were studied in detail previously, here we focus on the in-plane heat conduction. To analyze the relative contribution of electron transport to the in-plane heat conduction, we applied sheet-resistance measurements. Results of Mo/Si multilayers with variable thickness of the Mo layers indicate that the net in-plane thermal conductivity depends on the microstructure of the Mo layers. © *2015 AIP Publishing LLC*.
[http://dx.doi.org/10.1063/1.4928958]

INTRODUCTION

An important class of nanostructured materials for various applications is multilayer structures, composed of stacked thin films of nanometer thickness. Heat conduction in such "multilayers" attracted recently by interest due to the pronounced film-size effects and effects of scattering of heat carriers at interfaces on the overall thermal properties of such structures. For instance, the low cross-plane thermal conductivity in dielectric-dielectric or metal-dielectric multilayers is attractive for such applications as thermal insulation and thermo-electrics.[1–3] On the other hand, low cross-plane thermal conductivity of multilayer structures used as optical coatings for various applications can adversely affect its performance. This is especially critical for applications of extreme ultraviolet and soft X-ray multilayer mirrors, which are typically composed of nanometer-scale thin layers, i.e., layers thinner than typical mean free path of heat carriers in bulk materials.[4,5] Thermal transport in metal-metal multilayers is also a significant issue for the fundamental studies[6] and for a number of applications including heat-assisted magnetic recording,[7] spintronics,[8] and magnetic sensors.[9]

The layered structure of such materials induces an anisotropy of its transport properties, including heat conduction.[10] This is especially relevant for metal/dielectric or metal/semiconductor multilayers where transport of electrons across interfaces is strongly suppressed and thus its contribution to the net transport of heat can be low, but the in-plane heat transport can be dominated by electrons. As a result, in terms of the heat transport periodic multilayer structures can be treated as a uniaxial effective medium with distinctly different cross- and in-plane thermal conductivities. Most of the previous studies were focused on the cross-plane heat conduction mechanisms in metal/dielectric multilayer structures.[3,10–18] At the same time, studies of the in-plane heat conduction and the anisotropy of heat conduction were reported only by Li *et al.*[10,12] However, the in-plane thermal properties were measured in this work only for one multilayer structure. Furthermore, the main focus of their work was again on the understanding of mechanisms determining the cross-plane heat conduction.

In this paper, we report on the studies of anisotropic thermal properties of periodic Mo/Si multilayer structures with varied thickness of Mo layers in the nanometer range. Both cross- and in-plane thermal conductivity were measured. However, here we focus more on the interpretation of the in-plane thermal conductance. The thermal measurements were performed with a different technique, using the frequency domain thermoreflectance (FDTR).[19,20] Additionally, we analysed the in-plane electrical conductivity of the multilayers and this way estimated the electron contribution to the in-plane thermal conductivity.

EXPERIMENT

The multilayers were grown on superpolished fused silica substrates using dc magnetron sputtering in a turbomolecular pumped high vacuum deposition system with a base pressure of 10^{-8} mbar. The depositions were performed using Kr as the sputtering gas. The targets were sputtered in a constant power mode. The substrate holder was rotated to enable uniform deposition. The deposition of Mo and Si rates was calibrated using the deposition of single Mo and Si layers. The thicknesses of the layers during deposition were controlled by time. The actual layer thicknesses of the deposited structures were measured by hard X-ray grazing incidence reflectometry.

Parameters of Mo/Si studied multilayers are listed in Table I. The thickness of Si layers was fixed, and the thickness of Mo layers was varied. That allowed to vary the metal fraction and thus allowed to change the net in- and

[a)]Currently with Institute for Spectroscopy RAS, Troitsk, Moscow 142190, Russia.

TABLE I. Parameters of the studied multilayer samples and their measured values of electrical conductivity.

Sample	Number of periods	Si layer (nm)	Mo layer (nm)	$\sigma\ 10^6\ \Omega^{-1}\ m^{-1}$
Mo_2/Si_4	160	4 ± 0.04	2 ± 0.02	0.312 ± 0.005
Mo_4/Si_4	120	4 ± 0.04	4 ± 0.04	1.043 ± 0.044
Mo_6/Si_4	96	4 ± 0.04	6 ± 0.06	1.898 ± 0.040

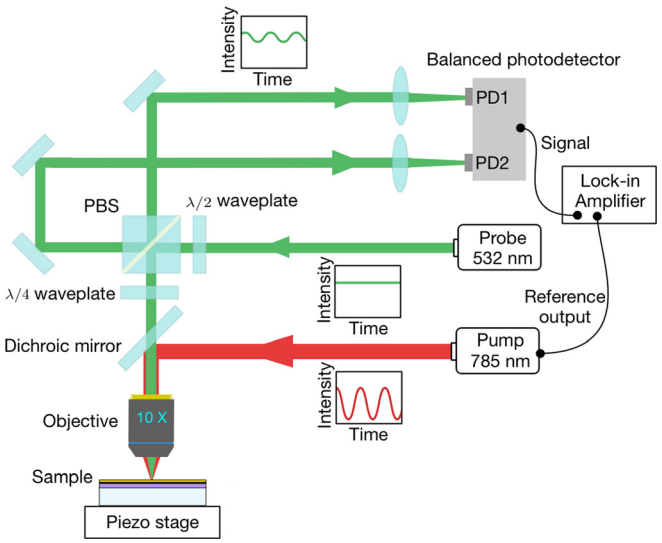

FIG. 1. Schematic of our FDTR microscope. A digitally modulated pump laser heats the sample while a probe beam monitors the surface reflectivity. A balanced photo detector is used to improve the signal to noise ratio.

cross-plane transport properties. Note that the overall thickness of the studied samples, i.e., (number of periods) × (Si thickness + Mo thickness) remained fixed.

Electrical conductivity of the described multilayer structures was measured by the four-point collinear probe method[21] using a "Cascade Microtech"® probe head with a probe spacing of 1.25 mm and a Keithley 2400 source meter. The probe tip radius was chosen to be 17.5 μm to ensure small point electrical contacts. The mean value for each sample was found by averaging 20 measurement results.

Fig. 1 shows our experimental setup for FDTR measurements which is based on two TEM00 free space continuous-wave lasers. A detailed description of the setup can be found in Ref. 20. Here, we briefly describe the working principle. A digitally modulated pump laser (785 nm) is focused through a 10× microscope objective to a Gaussian spot that locally heats a sample, while an unmodulated probe laser beam (532 nm) monitors the surface temperature through a proportional change in reflectivity. The focused pump and probe spot radii were determined to be 2.8 μm and 2.3 μm, respectively, by a knife-edge technique. A 50–100 nm thick metal layer that is usually referred to as transducer layer is coated on the sample to absorb the pump fluence and reflect the probe beam. The pump beam modulation frequency is typically varied from 10 kHz to 50 MHz, which enables high sensitivity for anisotropic measurements.[19] A radio-frequency lock-in amplifier records the amplitude and phase response of the reflected probe beam. Unknown thermal properties of the sample are then extracted based on a non-linear least squares routine, minimizing the error between the measured phase lag at each frequency and an analytical solution to the heat diffusion equation for a multilayer stack of materials. Our multilayer diffusion model calculates the frequency response of the surface temperature to the pump beam, and includes cross-plane and radial transport as well as the thermal boundary conductance (TBC) between each layer. An explicit expression of the model can be found in Ref. 22.

Prior to the measurements of thermal conductivity, the samples were coated with a 110 nm thick TiN film acting as the transducer layer. TiN was deposited using reactive magnetron sputtering of Ti in a mixture of Kr and N2. Two factors favored the choice of TiN as the transducer material. The first is the relatively low thermal conductivity of TiN as compared to those of standardly used transducers such as Au and Al. This enabled the increased heat accumulation in the Mo/Si multilayer structure and thus increased sensitivity for the in-plane measurements. Note that for the same reason we chose fused silica substrate instead of standardly used crystalline Si—its low thermal conductivity also enabled sensitivity for the in-plane measurements. The second factor is the large thermoreflectance dR/dT of TiN,[23] which results in an enhanced sensitivity for FDTR measurements.

The configuration of the multilayer sample, shown in Fig. 2(a), includes three layers: TiN transducer, multilayer, and fused silica substrate. Each layer is modeled with five physical parameters: the volumetric heat capacity, ρc_p, the cross- and in-plane thermal conductivities, $k_\perp$ and $k_\parallel$, the layer thickness, d, and the TBC to the next layer, G. We acquired FDTR phase data on the samples from the lock-in amplifier, and the cross- and in-plane thermal conductivities of the multilayer, $k_{ML,\perp}$ and $k_{ML,\parallel}$ were obtained by performing a two-parameter fit of our thermal diffusion model to the

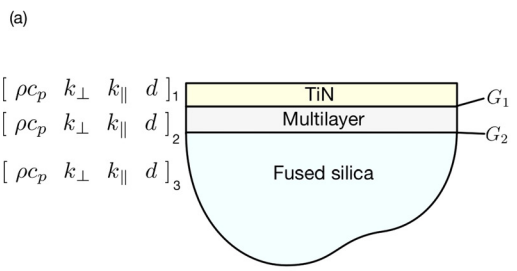

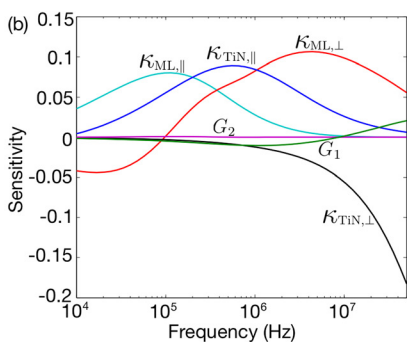

FIG. 2. (a) Sample configuration for FDTR measurements. (b) Calculated phase sensitivity to the cross- and in-plane thermal conductivities of the multilayer, $k_{ML,\perp}$ and $k_{ML,||}$, the cross- and in-plane thermal conductivities of TiN, $k_{TiN,\perp}$ and $k_{TiN,||}$, and the TBCs, G_1 and G_2.

phase data, after the properties of the other layers in the stack had been determined with additional measurements on reference samples. We used the bulk properties of the fused silica substrate from literature.[24] The volumetric heat capacity of the multilayer was used as the thickness weighted average of the bulk values of Si and Mo.[24] The volumetric heat capacity of TiN was also taken from literature.[25] Fig. 2(b) shows the measurement sensitivity, which is standardly determined as the partial derivative of the phase signal to a parameter in the model.[19] We have found from a scanning electron microscopy image of the cross section of the TiN film that TiN has a columnar structure that should have an effect on anisotropy of thermal conductivity. $k_{TiN,\perp}$ and $k_{TiN,||}$ of the TiN film were then measured by FDTR on a TiN/fused silica reference sample and obtained to be 20.4 ± 1 W m^{-1} K^{-1} and 11.7 ± 0.9 W m^{-1} K^{-1}, respectively, with the standard deviation of multiple measurements as the error bar. Note that the decreased due to the columnar structure in-plane thermal conductivity of TiN provides higher sensitivity for the in-plane measurements for the underlying multilayer structure with respect to our expectation in the assumption of standard thermal properties of bulk TiN. For the top and bottom TBCs of the multilayer, Fig. 2(b) shows that our measurement is insensitive to the bottom interface; therefore, we did not measure but instead used a typical value of 100 MW m^{-2} K^{-1} for a metal/dielectric interface as G_2.[26] The top interface G_1 was determined by depositing the same TiN film on a ~500 nm a-Si/fused silica reference sample and measuring the TBC between TiN and a-Si by FDTR. G_1 was then obtained to be 96 ± 26 MW m^{-2} K^{-1}.

RESULTS AND DISCUSSIONS

In Fig. 3, we show typical FDTR phase data for the three TiN coated multilayer samples and their best fit to the model. To determine the measurement uncertainty for these samples, we used a Monte Carlo method to account for the uncertainty caused by the physical parameters in our thermal model,[27] repeatedly fitting the data based on the distribution of model parameters to obtain the distribution of fitted values. Each parameter in our thermal model was assumed to have a normal distribution about its mean value with

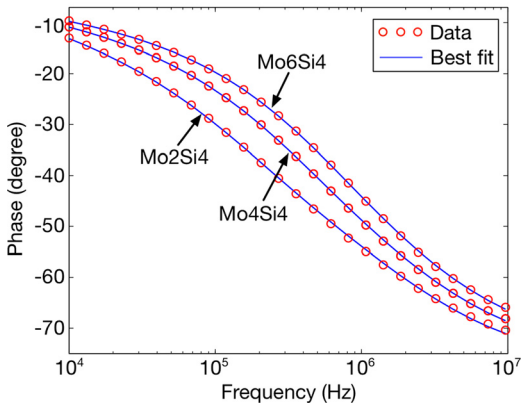

FIG. 3. FDTR measured phase signals and model best fit curves of the three TiN-coated multilayer samples.

standard deviation obtained from separate FDTR measurements. The FDTR data fitting were performed for 10 000 iterations. Within each iteration, our Matlab program randomly generates a value for every parameter based on their own distributions and performs the data fitting to the thermal model based on the parameters generated. The assembled histogram of the fitted values was then fitted to a normal distribution. We define the mean as the measured value and the standard deviation as the uncertainty. We also did five measurements on each sample at different locations and each phase data file was fitted for 2000 times using the Monte Carlo method. The total 10 000 values were combined to give the final measured value and uncertainty. This includes errors from both the experimental noise and physical properties. The cross- and in-plane thermal conductivity values for the three samples are summarized in Table II.

In order to analyze the cross-plane heat conduction, we applied a simplified thermal resistor model according to Eq. (1). Note that here and in the analysis of in-plane measurements we neglected the formation of silicides at interfaces

$$R_{\mathrm{Mo/Si}} = \frac{d_{\mathrm{MO}} + d_{\mathrm{Si}}}{k_{\perp}} = \frac{d_{\mathrm{MO}}}{k_{\mathrm{MO}}} + \frac{d_{\mathrm{Si}}}{k_{\mathrm{Si}}} + \frac{2}{G_{\mathrm{int}}}, \qquad (1)$$

where $k_{\perp}$ is the cross-plane thermal conductivity of the multilayer and k_{MO} and k_{Si} are the thermal conductivities of the Mo layer alone and the Si layer alone, respectively, d_{Mo} and d_{Si} are the Mo and Si layer thicknesses, respectively, and G_{int} is the averaged thermal boundary conductance. In the analysis, we used the value of $k_{\mathrm{Si}} = 1.01$ W m^{-1} K^{-1} that was measured by FDTR for 500 nm amorphous Si on fused silica substrate, while for Mo we estimated its thermal conductivity using the measured in-plane thermal conductivity data in the assumption of isotropic thermal conductivity of Mo layers. Eq. (1) was used to fit the measured $k_{\perp}$ data with G_{int} as the only free parameter, as shown in Fig. 4. The best fit is achieved with $G_{\mathrm{int}} = 550$ MW m^{-2} K^{-1}, similar to previously reported values for metal–nonmetal interfaces.[26] From Fig. 4, it is seen that the simplified thermal resistor model correctly describes the measured dependence of $k_{\perp}$ on the Mo layer thickness. This indicates the diffuse character of the cross-plane heat conduction, which is in good correspondence with previous studies.[10]

In order to analyze the contribution of electrons to the in-plane heat conduction, we applied the Wiedemann-Franz law to the measured electrical conductivities of the samples in order to estimate electron thermal conductivity $k_{\mathrm{e,WF}}$. In our calculations, we used the corrected Lorenz factor for Mo according to Stojanovic *et al.*[28] The calculated values for

TABLE II. Measured thermal conductivity values of Si/Mo multilayers.

Sample	$k_{\perp}$ (W m^{-1} K^{-1})	$k_{\|\|}$ (W m^{-1} K^{-1})	Anisotropy ratio $k_{\|\|}/k_{\perp}$
Mo_2/Si_4	0.75 ± 0.03	2.47 ± 0.14	3.3
Mo_4/Si_4	1 ± 0.03	8.48 ± 0.18	8.5
Mo_6/Si_4	1.3 ± 0.03	15.7 ± 0.24	12.1

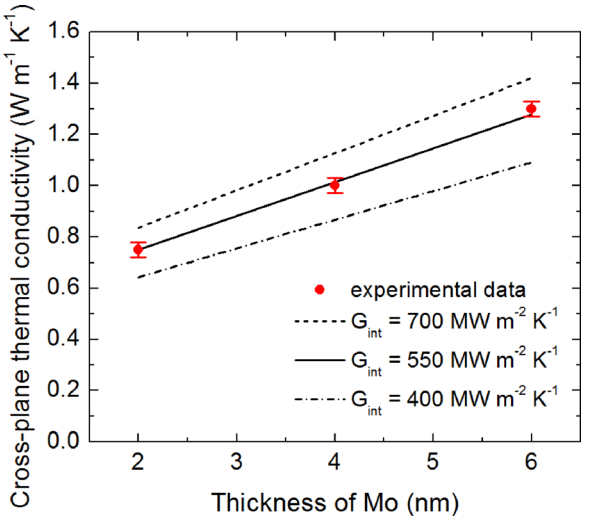

FIG. 4. Blue dots—measured cross-plane thermal conductivity. Lines—fitting with the thermal resistor model by changing the G_{int} value of Mo/Si.

$k_{\text{e,WF}}$ are given in Fig. 5(a) together with the FDTR measured $\kappa_{||}$ values. As it is seen from Fig. 5(a), the calculated $k_{\text{e,WF}}$ values are lower than those measured with FDTR technique. And it is also seen that the discrepancy $(k_{FDTR} - k_e)$ grows with the increase of the Mo thickness. The observed quantitative discrepancy between the measured $k_{||}$ and k_e might be ascribed to the phonon contribution to the in-plane heat conduction. In order to analyze this, we estimated the in-plane contribution of the lattice thermal conductivity for Si/Mo multilayer structure via

$$k_p = \frac{d_{Si}}{d_{Si} + d_{Mo}} k_{p,Si} + \frac{d_{Mo}}{d_{Si} + d_{Mo}} k_{p,Mo}, \tag{2}$$

where d_{Si} and d_{Mo} are Si and Mo layer thicknesses, respectively, and $k_{p,Si}$ and $k_{p,Mo}$ are phonon thermal conductivities of Si and Mo, respectively. For Si we again used the measured thermal conductivity value of 1.01 W m^{-1} K^{-1} since phonons are the main heat carrier in Si. The phonon thermal conductivity of Mo can be estimated by

$$k_{p,Mo} = \frac{1}{3} C_V v \lambda, \tag{3}$$

where C_V is the volumetric phonon heat capacity estimated using the Debye approximation, v is the speed of sound, and λ is the phonon mean free path in Mo. We used two different estimations for the phonon mean free path. In the first estimation, according to the minimum thermal conductivity theory,[29] the λ value was assigned to be equal to interatomic spacing in Mo, $a \approx 0.31$ nm.[24] In the second estimation, we used Matthiessen's rule[29] to calculate λ taking into account the thin film size effect via the following equation:

$$\frac{1}{\lambda} = \frac{1}{\lambda_{Bulk}} + \frac{1}{d}, \tag{4}$$

where λ_{Bulk} is the bulk mean free path and d is the film thickness. Here, λ_{Bulk} was calculated using the bulk phonon thermal conductivity of Mo extracted from the net thermal conductivity via the Wiedemann-Franz law. The first estimation is usually applied to amorphous thin films, while the second is more appropriate for poly-crystalline thin films. Note that in the first estimation we neglect the influence of the Mo amorphisation on its heat capacity. These two approaches were used because previously we observed that in Mo/Si multilayers the microstructure of Mo films, i.e., the ratio between crystalline and amorphous phases, is dependent on its thickness.[30] Mo films of about 2 nm thickness and thinner are fully composed of the amorphous phase.[30] The net estimated thermal conductivity composed of the phonon contribution calculated using Eqs. (2) and (3) and the electron contribution calculated using Wiedemann-Franz law is also given in Fig. 5(b). From Fig. 5(b) it is seen that for the Mo_2/Si_4 multilayer structure the measured value of thermal conductivity matches the net k value of phonon contribution *kp* estimated via the minimum thermal conductivity limit. The *kp* value calculated using the Matthiessen's rule overestimates the phonon contribution by about 1 W/m K. On the other hand, for the Mo_6/Si_4 multilayer the measured value of thermal conductivity matches the net *k* value of the phonon

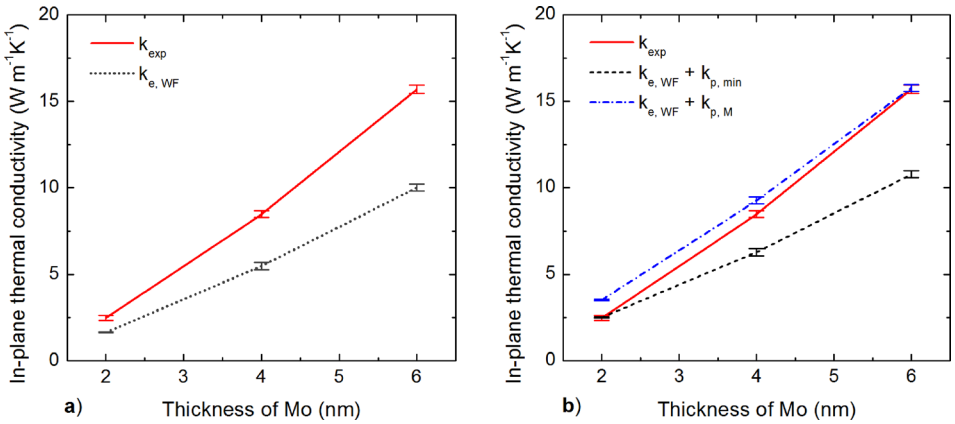

FIG. 5. (a) Red—measured in-plane thermal conductivity (denoted as k_{exp}) for the samples listed in Table I; grey—electron contribution to the in-plane thermal conductivity estimated via the Wiedemann-Franz law (denoted as $k_{e,WF}$). (b) Red—measured in-plane thermal conductivity; black—electron contribution to the in-plane thermal conductivity together with phonon contribution estimated via the minimum thermal conductivity limit in the assumption of amorphous Mo layers (denoted as $k_{e,WF} + k_{p,\text{min}}$); blue—electron contribution to the in-plane thermal conductivity together with phonon contribution estimated using the Matthiessen's rule in the assumption of crystalline Mo layers (denoted as $k_{e,WF} + k_{p,M}$).

contribution estimated assuming crystalline Mo layers. In this case, the minimum thermal conductivity limit underestimates the phonon contribution by 5 W/m K. For the Mo_4/Si_4 multilayer structure, the experimental value is closer to the net k value calculated using the Matthiessen's rule than to the value calculated using the alternative approach. The observed discrepancy of about 0.8 W/m K can be explained here by, e.g., a non-negligible fraction of amorphous material in the Mo layers. These considerations bring us to the conclusion that the microstructure of the thin film metal layers, i.e., the ratio between crystalline and amorphous phases, can strongly influence the lateral heat conduction in metal-dielectric and metal-semiconductor multilayers. Let us also note that the amorphisation effects can also influence the cross-plane thermal conductivity as it was shown for amorphous/crystalline Si multilayer structures.[31] But these effects are beyond the scope of this paper and required more detailed study.

CONCLUSIONS

We studied the anisotropic heat conduction in periodic nanoscale Mo/Si multilayered films using the pump-probe FDTR technique. The structures analyzed, each having a fixed thickness of the Si layers of 4 nm and a varied thickness of the Mo layers in the 2–6 nm range, demonstrate a measured anisotropy ratio $\kappa_{\parallel}/\kappa_{\perp}$ ranging from 3.3 for 2 nm to 12.1 for 6 nm layers. The variation of metal layer thickness has a significantly higher impact on the in-plane heat conduction than on the cross-plane heat conduction. This is so because the lateral electron transport along the metal layers contributes to the in-plane heat conduction proportionally to the thickness of metal layers, while the cross-plane transport for such multilayer structures is dominated by lattice vibrations and its scattering at interfaces. The measured in-plane thermal conductivity was in good agreement with calculations taking into account both electron and phonon thermal transport, using a phonon mean free path which depended on the Mo layer thickness. Based on the previously gained knowledge on Mo microstructure in Mo/Si multilayers, we suggest that the ratio between crystalline and amorphous phases in the metal layers affects the in-plane heat conduction. Namely, reducing the Mo layer thickness down to 2 nm, the in-plane heat conduction decreases due to amorphization of the Mo layers. Finally, it was shown that FDTR technique can be used successfully for characterizing the thermal conductivity tensor of multilayer structures without complex sample preparation.

ACKNOWLEDGMENTS

This work is part of the research program "Controlling photon and plasma induced processes at EUV optical surfaces (CP3E)" of the "Stichting voor Fundamenteel Onderzoek der Materie (FOM)" which is financially supported by the Nederlandse Organisatie voor Wetenschappelijk Onderzoek (NWO). The CP3E programme is cofinanced by Carl Zeiss SMT GmbH (Oberkochen), ASML (Veldhoven), and the Agentschap NL through the Catrene EXEPT program. The work was additionally supported by the XUV Optics consortium with funding by the Province of Overijssel, the MESA+ Institute for Nanotechnology, ASML, Carl Zeiss SMT AG, PANalytical, DEMCON and Solmates.

[1]B. Yang, J. L. Liu, K. L. Wang, and G. Chen, "Simultaneous measurements of Seebeck coefficient and thermal conductivity across superlattice," Appl. Phys. Lett. **80**, 1758–1760 (2002).
[2]A. Kyarad and H. Lengfellner, "Al–Si multilayers: A synthetic material with large thermoelectric anisotropy," Appl. Phys. Lett. **85**, 5613–5615 (2004).
[3]R. M. Costescu, D. G. Cahill, F. H. Fabreguette, Z. A. Sechrist, and S. M. George, "Ultra-low thermal conductivity in W/Al_2O_3 nanolaminates," Science **303**, 989–990 (2004).
[4]A. R. Khorsand, R. Sobierajski, E. Louis, S. Bruijn, E. D. van Hattum, R. W. E. van de Kruijs, M. Jurek, D. Klinger, J. B. Pelka, L. Juha, T. Burian, J. Chalupsky, J. Cihelka, V. Hajkova, L. Vysin, U. Jastrow, N. Stojanovic, S. Toleikis, H. Wabnitz, K. Tiedtke, K. Sokolowski-Tinten, U. Shymanovich, J. Krzywinski, S. Hau-Riege, R. London, A. Gleeson, E. M. Gullikson, and F. Bijkerk, "Single shot damage mechanism of Mo/Si multilayer optics under intense pulsed XUV-exposure," Opt. Express **18**, 700–712 (2010).
[5]M. Müller, F. Barkusky, T. Feigl, and K. Mann, "EUV damage threshold measurements of Mo/Si multilayer mirrors," Appl. Phys. A **108**, 263–267 (2012).
[6]R. B. Wilson and D. G. Cahill, "Experimental validation of the interfacial form of the Wiedemann-Franz law," Phys. Rev. Lett. **108**, 255901 (2012).
[7]T. W. McDaniel, "Ultimate limits to thermally assisted magnetic recording," J. Phys.: Condens. Matter **17**, R315 (2005).
[8]J. Bass and W. P. Pratt, Jr., "Spin-diffusion lengths in metals and alloys, and spin-flipping at metal/metal interfaces: an experimentalist's critical review," J. Phys.: Condens. Matter **19**, 183201 (2007).
[9]J. M. Daughton, "GMR applications," J. Magn. Magn. Mater. **192**, 334–342 (1999).
[10]Z. Li, S. Tan, E. Bozorg-Grayeli, T. Kodama, M. Asheghi, G. Delgado, M. Panzer, A. Pokrovsky, D. Wack, and K. E. Goodson, "Phonon dominated heat conduction normal to Mo/Si multilayers with period below 10 nm," Nano Lett. **12**, 3121–3126 (2012).
[11]E. Dechaumphai, D. Lu, J. J. Kan, J. Moon, E. E. Fullerton, Z. Liu, and R. Chen, "Ultralow thermal conductivity of multilayers with highly dissimilar debye temperatures," Nano Lett. **14**, 2448–2455 (2014).
[12]E. Bozorg-Grayeli, Z. Li, M. Asheghi, G. Delgado, A. Pokrovsky, M. Panzer, D. Wack, and K. E. Goodson, "Thermal conduction properties of Mo/Si multilayers for extreme ultraviolet optics," J. Appl. Phys. **112**, 083504 (2012).
[13]Y. Ju, M.-T. Hung, and T. Usui, "Nanoscale heat conduction across metal-dielectric interfaces," J. Heat Transfer **128**, 919–925 (2006).
[14]F. Döring, C. Eberl, S. Schlenkrich, F. Schlenkrich, S. Hoffmann, T. Liese, H. U. Krebs, S. Pisana, T. Santos, H. Schuhmann, M. Seibt, M. Mansurova, H. Ulrichs, V. Zbarsky, and M. Münzenberg, "Phonon localization in ultrathin layered structures," Appl. Phys. A **119**, 11–18 (2015).
[15]J. Lombard, F. Detcheverry, and S. Merabia, "Influence of the electron–phonon interfacial conductance on the thermal transport at metal/dielectric interfaces," J. Phys.: Condens. Matter **27**, 015007 (2015).
[16]Y. S. Ju, M.-T. Hung, M. J. Carey, M.-C. Cyrille, and J. R. Childress, "Nanoscale heat conduction across tunnel junctions," Appl. Phys. Lett. **86**, 203113 (2005).
[17]V. Rawat, Y. K. Koh, D. G. Cahill, and T. D. Sands, "Thermal conductivity of (Zr,W)N/ScN metal/semiconductor multilayers and superlattices," J. Appl. Phys. **105**, 024909 (2009).
[18]B. Saha, T. D. Sands, and U. V. Waghmare, "First-principles analysis of ZrN/ScN metal/semiconductor superlattices for thermoelectric energy conversion," J. Appl. Phys. **109**, 083717 (2011).
[19]A. J. Schmidt, R. Cheaito, and M. Chiesa, "A frequency-domain thermoreflectance method for the characterization of thermal properties," Rev. Sci. Instrum. **80**, 094901 (2009).
[20]J. Yang, C. Maragliano, and A. J. Schmidt, "Thermal property microscopy with frequency domain thermoreflectance," Rev. Sci. Instrum. **84**(10), 104904 (2013).
[21]D. K. Schroder, *Semiconductor Material and Device Characterization*, 3rd ed. (Wiley-IEEE Press, 2006).
[22]A. Feldman, "Algorithm for solutions of the thermal diffusion equation in a stratified medium with a modulated heating source," High Temp. - High Pressures **31**(3), 293–298 (1999).

[23]R. M. Costescu, M. A. Wall, and D. G. Cahill, "Thermal conductance of epitaxial interfaces," Phys. Rev. B **67**, 054302 (2003).
[24]D. R. Lide, *CRC Handbook of Chemistry and Physics*, edited by D. R. Lide (Taylor & Francis, Boca Raton, FL, 2007).
[25]H. O. Pierson, *Handbook of Refractory Carbides and Nitrides: Properties, Characteristics, Processing and Applications* (Noyes Publications, 1996).
[26]R. J. Stevens, A. N. Smith, and P. M. Norris, "Measurement of thermal boundary conductance of a series of metal-dielectric interfaces by the transient thermoreflectance technique," J. Heat Transfer **127**(3), 315 (2005).
[27]W. Navidi, *Statistics for Engineers and Scientists* (McGraw-Hill, 2010).
[28]N. Stojanovic, D. H. S. Maithripala, J. M. Berg, and M. Holtz, "Thermal conductivity in metallic nanostructures at high temperature: Electrons, phonons, and the Wiedemann-Franz law," Phys. Rev. B **82**, 075418 (2010).
[29]T. M. Tritt, *Thermal Conductivity: Theory, Properties, and Applications* (Kluwer Academic/Plenum Publishers, New York, 2004).
[30]R. W. E. van de Kruijs, E. Zoethout, A. E. Yakshin, I. Nedelcu, E. Louis, H. Enkisch, G. Sipos, S. Müllender, and F. Bijkerk, "Nano-size crystallites in Mo/Si multilayer optics," Thin Solid Films **515**, 430–433 (2006).
[31]A. France-Lanord, S. Merabia, T. Albaret, D. Lacroix, and K. Termentzidis, "Thermal properties of amorphous/crystalline silicon superlattices," J. Phys.: Condens. Matter **26**, 355801 (2014).